Antiviral Research 161 (2019) 36–45

Contents lists available at ScienceDirect

Antiviral Research

journal homepage: www.elsevier.com/locate/antiviral

5′-triphosphate siRNA targeting HBx elicits a potent anti-HBV immune response in pAAV-HBV transfected mice

Qiuju Han[a], Zhaohua Hou[b], Chunlai Yin[a], Cai Zhang[a], Jian Zhang[a,*]

[a] Institute of Immunopharmaceutical Sciences, School of Pharmaceutical Sciences, Shandong University, 44 Wenhua West Road, Jinan 250012, China
[b] Laboratory of Immunology for Environment and Health, Shandong Analysis and Test Center, Qilu University of Technology (Shandong Academy of Sciences), 19 Keyuan Road, Jinan 250014, China

ARTICLE INFO

Keywords:
HBV
RNA interference
Immunotherapy
RIG-I

ABSTRACT

RNA with 5′-triphosphate (3p-RNA) is recognized by RNA sensor RIG-I (retinoic acid–inducible gene I protein). Previously, we reported that small interfering RNA targeting HBx (3p-siHBx) could confer potent anti–hepatitis B virus (HBV) efficacy via HBx silencing and RIG-I activation. However, the characteristics of innate and adaptive immunity especially exhaustion profiles in the liver microenvironment in response to 3p-siHBx therapy have not been fully elucidated. Here, we observed that 3p-siHBx more significantly inhibited HBV replication *in vivo*. 3p-siHBx enhanced natural killer (NK) cell activation with KLRG1 and CD69 upregulation and interferon (IFN)-γ secretion. 3p-siHBx significantly reversed the exhaustion phenotype of $CD8^+$ T cells, and augmented $CD8^+$ T cell activation and function. Importantly, 3p-siHBx disrupted the differentiation of myeloid-derived suppressor cells (MDSC) and regulatory T cells (Treg), accompanied by the reduction of the immunosuppressive cytokines interleukin (IL)-10 and transforming growth factor (TGF)-β. 3p-siHBx also enhanced dendritic cell maturation. Further investigation showed that RIG-I was involved in 3p-siHBx–induced IFN-α, IFN-β, and IFN-λ production. Moreover, RIG-I activation in HBV^+ hepatocytes would improve the recruitment of $CD8^+$ T cells and NK cells. These results reveal that 3p-siHBx therapy can improve the immune microenvironment in HBV-carrier liver and inhibit HBV replication, indicating the potential utility of RIG-I ligands as molecular adjuvants for viral vaccines or candidate drugs.

1. Introduction

RNA interference (RNAi) is a conserved mechanism against exogenous nucleic acid and transposon transcripts in organisms ranging from nematodes to humans, which is mediated by short double-stranded (ds) RNAs usually 21 or 22 nucleotides in length (Elbashir et al., 2001). The great potential of RNAi is the specific repression of the expression of disease-causing genes.

Recently, anti-tumor or antiviral strategies using RNAi for both gene silencing and innate-receptor activation were designed; one mechanism of these strategies is activating the intracellular retinoic acid–inducible gene I protein (RIG-I). 5′-Triphosphate RNA (3p-small interfering RNA [siRNA]) is the exact molecular feature of RNA required for RIG-I recognition, and acts as a RIG-I agonist (Schlee et al., 2009; Schmidt et al., 2009). Upon ligand binding, RIG-I initiates a specific signaling cascade and results in the activation of transcription factors such as interferon (IFN) regulatory factor (IRF)-3, IRF-7, and nuclear factor (NF)-κB, depending on the adaptor protein mitochondrial antiviral signaling protein (MAVS, also known as IPS-1, VISA, or Cardif). RIG-I signaling triggers the potent induction of a set of genes, including type I IFN, IFN-stimulated genes (ISGs), and the chemokine CXCL10 (Kell and Gale, 2015; Yoneyama and Fujita, 2009). Based on these findings, bifunctional 3p-siRNAs combining RIG-I–mediated immune activation with target gene silencing have been designed within a single molecule as a novel 3p-siRNA therapeutic strategy.

Early in 2005, Poeck et al. reported that bifunctional 3p-siRNAs targeting Bcl-2 led to better melanoma tumor reduction than OH-siRNA or 5′-triphosphate siRNAs containing target mismatches (Poeck et al.,

Abbreviations: RNAi, RNA interference; HBV, hepatitis B virus; dsRNA, double-stranded (ds) RNAs; RIG-I, retinoic acid inducible gene I; PRRs, pathogen recognition receptors; IFN, interferon; ISG, interferon stimulated gene; HBsAg, hepatitis B surface antigen; HBeAg, hepatitis B e antigen; HBcAg, hepatitis B core antigen; MDA-5, melanoma differentiation-associated gene 5; MAVS, mitochondrial antiviral signaling protein; RIG-G, retinoic acid inducible gene G; H&E, Hematoxylin-eosin staining; FACS, Fluorescence activated cell sorter; ELISA, enzyme-linked immunosorbent assay; FBS, fetal bovine serum; GAPDH, glyceraldehyde 3-phosphate dehydrogenase; OAS, 2′-5′oligoadenylate synthetase

* Corresponding author.
E-mail address: zhangj65@sdu.edu.cn (J. Zhang).

https://doi.org/10.1016/j.antiviral.2018.11.006
Received 17 January 2018; Received in revised form 2 October 2018; Accepted 14 November 2018
Available online 15 November 2018
0166-3542/

2008). Subsequently, bifunctional 3p-siRNAs targeting the transforming growth factor β1 (*TGFB1*), survivin (*BIRC5*), glutaminase (*GLS*), and vascular endothelial growth factor (*VEGF*) genes were designed, and provoked massive apoptosis of tumor cells and induced more prominent anti-tumor responses in different tumor models (Ellermeier et al., 2013; Meng et al., 2014; Wang et al., 2013; Yuan et al., 2015). These processes required the RIG-I–mediated type I IFN response. In a pancreatic cancer model, 3p-siRNA-TGFβ1 induced high levels of type I IFN and CXCL10, which led to the infiltration of activated $CD8^+$ T cells to the tumor tissue, while the frequency of $CD11b^+Gr\text{-}1^+$ myeloid cells was reduced (Ellermeier et al., 2013). Recently, it was shown that RIG-I activation induced by 3p-siRNAs could block the suppressive function of regulatory T cells (Tregs) and myeloid-derived suppressor cells (MDSCs) (Anz et al., 2010).

We and others have previously demonstrated that 3p-siRNAs against hepatitis B virus (HBV), influenza A virus, and coxsackievirus could elicit potent antiviral effects through gene silencing and RIG-I activation. Virus-specific 3p-siRNA could activate the RIG-I–mediated IFN-β pathway and significantly reduce viral load and virus-induced pathogenesis (Ahn et al., 2012; Chen et al., 2013; Ebert et al., 2011; Han et al., 2011; Lin et al., 2012). In primary HBV^+ hepatocytes, 5′-triphosphate-siRNA against HBx gene (3p-siHBx) inhibited HBV replication more strongly and promoted IFN production compared to siHBx, and this effect was mediated by RIG-I activation (Chen et al., 2013; Ebert et al., 2011; Han et al., 2011). However, during chronic HBV infection, the adaptive and innate immunity exhibit functional deficiency. In the case of natural killer (NK) cells, the percentage and expression of activating receptors are reduced, while inhibitory molecules are upregulated, and the capacity for producing cytokines such as IFN-γ and tumor necrosis factor (TNF)-α is impaired (Wu et al., 2015; Yang et al., 2017). As RIG-I activation is crucial for initiating antiviral innate responses and activating adaptive immunity, whether 3p-siHBx can reverse immune tolerance and improve the liver immune microenvironment is therefore worth investigating.

In this study, we analyzed the characteristics of liver immunity in response to 3p-siHBx treatment. And we found 3p-siHBx triggered NK cell and $CD8^+$ T cell activation in HBV-carrier mice, and decreased negative regulatory cells and cytokines. Furthermore, 3p-siHBx promoted type I IFN production mediated by RIG-I activation, inhibiting HBV replication and inducing immune response. This study provides *in vivo* evidence for the potential of 3p-siHBx in anti-HBV strategies.

2. Material and methods

2.1. HBV Carrier mouse model

HBV-carrier mice were established as previously described by P-J Chen's lab (Huang et al., 2006). Briefly, the pAAV/HBV1.2 vector (kindly provided by Pei-Jer Chen, National Taiwan University College) was delivered into C57BL/6 mice using the hydrodynamic tail vein injection method. After 4 weeks, the serum was collected, and the hepatitis B surface antigen (HBsAg) level was assayed. HBV-carrier mice (HBV^+) were defined as harboring serum HBsAg levels > 500 ng/mL. All animals were kept under standard laboratory conditions and provided with food and water ad libitum. The animal experiments were approved by the Research Ethics Committee of Shandong University.

2.2. siHBx and 3p-siHBx treatment

siHBx was obtained from RiboBio (Guangzhou, China, Supplementary Table 1). 3p-scramble and 3p-siHBx were prepared using *in vitro* Transcription T7 Kit (Cat#6140, Takara, Dalian, China); the DNA templates (Supplementary Table 2) were synthesized by Beijing Genomics Institute (Beijing, China). For *in vivo* administration, 50 μg RNA complexed with 1, 2-dioleoyl-3-trimethylammonium-propane (DOTAP, Cat#144189-73-1, Roche Life Science) was injected via the tail vein three times every 2 days.

2.3. HBV DNA and pgRNA assay

HBV copies were detected by quantitative PCR (qPCR) using a HBV DNA assay kit (Da An Gene, Guangzhou, China) according to the manufacturer's instructions. The level of pgRNA was detected by qPCR, and the primers was list in (Supplementary Table 3).

2.4. Enzyme-linked immunosorbent assay (ELISA)

Serum and liver protein lysate were collected, and the levels of IFN-α, IFN-β, TGF-β, and IL-10 levels were determined using ELISA kits (Cusabio, Wuhan, China) according to the manufacturer's specifications. ELISA kits were also used to assay anti-HBs (Cat#S10980089, Wantai Bio-pharm, Beijing, China) and HBsAg (Cat# A2000, Antobio, Zhengzhou, China) according to the manufacturers' instructions.

2.5. Hematoxylin–eosin staining (H&E)

Two weeks after the last RNA treatment, the mice were sacrificed, and mouse liver sections were embedded. Then, formalin-fixed and paraffin-embedded liver tissues were stained with H&E for histological investigations to evaluate the degree of liver injury, which was based on necrotic lesion severity in the liver parenchyma. Then, liver histological changes such as hepatocyte lesions and liver structural changes were evaluated.

2.6. Immunohistochemistry (IHC)

Two weeks after the last RNA treatment, the mice were sacrificed, and mouse liver sections were embedded. Paraffin-embedded and formalin-fixed mouse liver samples were cut into 5-μm sections and processed for IHC as described previously (Lan et al., 2013). After incubation with antibody against hepatitis B core antigen (HBcAg) overnight at 4 °C (Cat#A2000, Genetech, Shanghai, China), the signal was developed with an EnVision™ detection kit (Cat#GK500705, Genetech).

2.7. Fluorescence-activated cell sorting (FACS)

Intrahepatic lymphocytes were isolated as previously described (Lan et al., 2013), then stained with peridinin chlorophyll protein (PerCP)-Cy5.5–conjugated anti-CD3(Cat#35-0031-82), fluorescein isothiocyanate (FITC)-conjugated anti-NK1.1 (Cat#11-5941-82), PerCP-eFluor 710–conjugated anti-CD27 (Cat#46-0271-82), phycoerythrin (PE)-conjugated anti-CD69 (Cat#12-0691-82), FITC-conjugated anti-CD11c (Cat#11-0114-82), PE-conjugated anti-NKG2A (Cat#12-5897-81), PE-conjugated anti-NKG2D (Cat#12-5882-82), or isotype-matched controls (eBioscience, San Diego, CA). For intracellular staining, the cells were first stained with surface markers, fixed and permeabilized, followed by intracellular staining for IFN-γ with PE-conjugated anti−IFN−γ (Cat#25-7311-82, eBioscience). Cells were acquired on a FACSCalibur flow cytometer or FACSAria II cell sorter (BD), and analyzed using WinMDI analysis software and FlowJo.

2.8. RNA extraction and PCR gene expression

Total RNA was extracted from liver tissues using TRIzol (Cat#15596026, Invitrogen Life Technologies) according to the manufacturer's instructions. Complementary DNA (cDNA) was synthesized with Moloney murine leukemia virus (Cat#M350B, M-MLV, Promega, Madison, WI). Quantitative real-time PCR was performed using SYBR Green master mix (Cat# 4707516001, Roche, Indianapolis, IN). All reactions were run in triplicate and the housekeeping gene glyceraldehyde-3-phosphate dehydrogenase (*GAPDH*) was amplified in a

parallel reaction for normalization. Supporting Table 3 lists the HBx, IFN-λ, IRF-7, and 2′-5′-oligoadenylate synthetase (OAS) primers used.

2.9. Western blotting

Liver samples were homogenized using radioimmunoprecipitation assay (RIPA) lysis buffer with protease inhibitor cocktail (Cat#P0013B, Beyotime Biotechnology, Shanghai, China). Protein (30 μg) was separated on 10% sodium dodecyl sulfate (SDS)-polyacrylamide gel. The proteins were transferred onto polyvinylidene fluoride (PVDF) membranes, and the blots were incubated for 1 h in blocking buffer containing 5% milk before being incubated with anti–RIG-I (Cat#4200), anti–extracellular signal–regulated kinase (ERK) (Cat#4695), or anti–β-actin rabbit monoclonal antibody (Cat#3700) (1:2000, Cell Signaling Technology, Danvers, MA) overnight at 4 °C, and subsequently treated with peroxidase-conjugated goat anti-rabbit immunoglobulin G (IgG) (Cat#57100, Dako, Carpentaria, CA) for 1 h at room temperature. Protein bands were visualized by enhanced chemiluminescence (ECL) (Cat#0000367, Millipore, Billerica, MA, USA) and analyzed by ImageLab software (Version 3.0, Bio-Rad).

2.10. MDSC isolation and flow cytometry analysis

MDSCs characterized as $CD11b^+Gr\text{-}1^+$ were sorted from freshly obtained intrahepatic mononuclear cells with the FACSAria II cell sorter (BD). Multicolor cell analysis was performed using FITC-conjugated anti-CD11b (Cat#11-0112-82), PE-conjugated anti–Gr-1 (Cat# 12-5931-82), and allophycocyanin (APC)-conjugated anti–inducible nitric oxide synthase (iNOS) (Cat#17-5920-82) (eBioscience). Cell surface and intracellular staining were performed as indicated in the manufacturer's data sheet.

2.11. Transwell invasion assay

HepG2. 2.15 cells (an HBV genomic DNA–transfected cell line) were transfected with 3p-siHBx, 3p-scramble or siHBx; 24 h later, the supernatant was collected. The cell migration assay was performed using 24-well Transwell plates containing 8-μm pore size polycarbonate filters (Corning Costar, Cambridge, MA). Peripheral blood mononuclear cells (PBMCs) isolated using Ficoll-Paque were placed in the top chamber, while the supernatant from HepG2. 2.15 cells treated with different types of siRNA were placed in the bottom chamber. The migrated cells were stained with crystal violet for image capture and counted under a light microscope. The percentages of immune cell subsets in the bottom chamber were determined by flow cytometry.

2.12. Statistical analysis

Data are presented as the mean ± SD (*in vitro* data) or mean ± SEM (*in vivo* data). Significant differences were analyzed using Student *t*-test or one-way analysis of variance (ANOVA) followed by Tukey's post-hoc test. Statistical analysis was conducted using GraphPad Prism (version 5.0a); $P < 0.05$ was considered significant.

3. Results

3.1. 3p-siHBx inhibited HBV replication in HBV-Carrier mice

To evaluate the potential anti-HBV effects of 3p-siHBx *in vivo*, HBV-carrier mice were established as described previously (Lan et al., 2013), and the conventional siRNA targeting HBx carrying a free 5-OH group (siHBx), non-targeting 5′-triphosphate siRNA (3p-scramble) and 3p-siHBx (50 μg) were hydrodynamically injected three times into HBV-carrier mice, respectively (Fig. 1A). As shown in Fig. 1B, both siHBx and 3p-siHBx showed inhibition of HBx and pgRNA in the liver tissue, compared with the DOTAP-treated control group (CTRL). HBsAg and HBV DNA levels in the serum were also markedly suppressed in a time-dependent manner compared to the CTRL mice (Fig. 1C and D). Most importantly, 3p-siHBx exhibited stronger anti- HBV effect than the conventional siHBx, while the irrelevant 3p-scramble only showed slight inhibitory effect on HBV in HBV carrier mice (Fig. 1B–D). Furthermore, histological examination of liver tissue sections by IHC revealed an obvious reduction of HBcAg by 3p-siHBx (Fig. 1E). HBsAb was not detectable in the serum of 3p-siHBx-treated mice (Supplementary Table 4). The anti-viral effect of 3p-siHBx treatment could last for three weeks (sFig. 1). In addition, 3p-siHBx or siHBx treatment did not elevate serum alanine aminotransferase (ALT) and aspartate aminotransferase (AST) levels compared with the CTRL mice (sFig. 2A), nor was significant necrosis observed in the 3p-siHBx-treated mice (sFig. 2B). Therefore, these results indicate that 3p-siHBx is more effective than conventional siHBx for inhibition of HBV replication without liver injury.

3.2. NK cell function was significantly activated in 3p-siHBx–treated HBV-Carrier mice

Innate immune response is disrupted during chronic HBV infection (Schuch et al., 2014; Yang et al., 2017). As shown in sFig. 3A, HBV-carrier mice (HBV +) had lower numbers of liver mononuclear cells than HBV- mice. Notably, NK cell number was also decreased in the liver in HBV-carrier mice (sFig. 3B), and there was increased NKG2A expression (sFig. 3C) and reduced CD107a and IFN-γ (sFig. 3E&F). Given the critical antiviral role of NK cells, we wanted to know whether 3p-scramble, siHBx or 3p-siHBx could affect NK cell maturation in the liver. We found that the liver of 3p-siHBx–treated mice had increased frequency and total number of fully activated NK cells ($CD11b^{high}CD27^{low}$) compared to CTRL mice (Fig. 2A&B), accompanied by elevated expression of KLRG1 and CD69, which are markers of NK cell cytotoxic activity (Fig. 2C&D). Importantly, 3p-siHBx also augmented the ability of NK cells to produce IFN-γ (Fig. 2E), which was accompanied by increased serum IFN-γ (Fig. 2F). Meanwhile, we observed the irrelevant 3p-scramble could activate NK cells, which was similar to the effect of 3p-siHBx, while the stimulatory effect of conventional siHBx was lower than 3p-RNA (Fig. 2C–F). These data suggest that 3p-siHBx promotes NK cell maturation and activation in HBV-carrier mice.

3.3. 3p-siHBx reactivated $CD8^+$ T cell function in HBV-Carrier mice

Chronic HBV infection causes defective adaptive immunity (de Niet et al., 2016). Here, we detected a marked reduction in $CD8^+$ T cells 4 weeks after pAAV/HBV1.2 injection, whereas $CD4^+$ T cells were not affected significantly (Fig. 3A&B). Via 3p-siHBx therapy, a potent immune activation was observed, as evidenced by strong upregulated CD69 expression on $CD8^+$ T cells in the livers of the HBV-carrier mice (Fig. 3C). 3p-siHBx also enhanced the ability of $CD8^+$ T cells to produce IFN-γ and TNF-α (Fig. 3D&E). In addition, we observed a 20% reduction in the Treg proportion by 3p-siHBx (Fig. 3F). Furthermore, PD-1 (programmed cell death protein 1), but not CTLA-4 (cytotoxic T-lymphocyte associated protein 4), was decreased on $CD8^+$ T cells in the livers from HBV-carrier mice 7 days after 3p-siHBx treatment (Figs. 3G and H). Although CD69 and TNF-α on $CD8^+$ T cells were increased by the administration of irrelevant 3p-scramble (Fig. 3C–E), the proportion of Treg and the expression of PD-1 and CTLA-4 were not affected significantly. Additionally, we observed that siHBx treatment slightly promoted the activation of CD8 + T cells (Fig. 3C–E), but significantly decreased the proportion of Treg and the expression of PD-1 (Fig. 3F–H). The irrelevant 3p-scramble treatment resulted in $CD8^+$ cell activation with upregulation of CD69, IFN-γ and TNF-α, which is similar to the effect of 3p-siHBx (Fig. 3C–E). Unlike 3p-siHBx, 3p-scramble has no significant effect on Treg and PD-1 (Fig. 3F–H). Therefore, 3p-siHBx induces $CD8^+$ T cell activation by reversing $CD8^+$

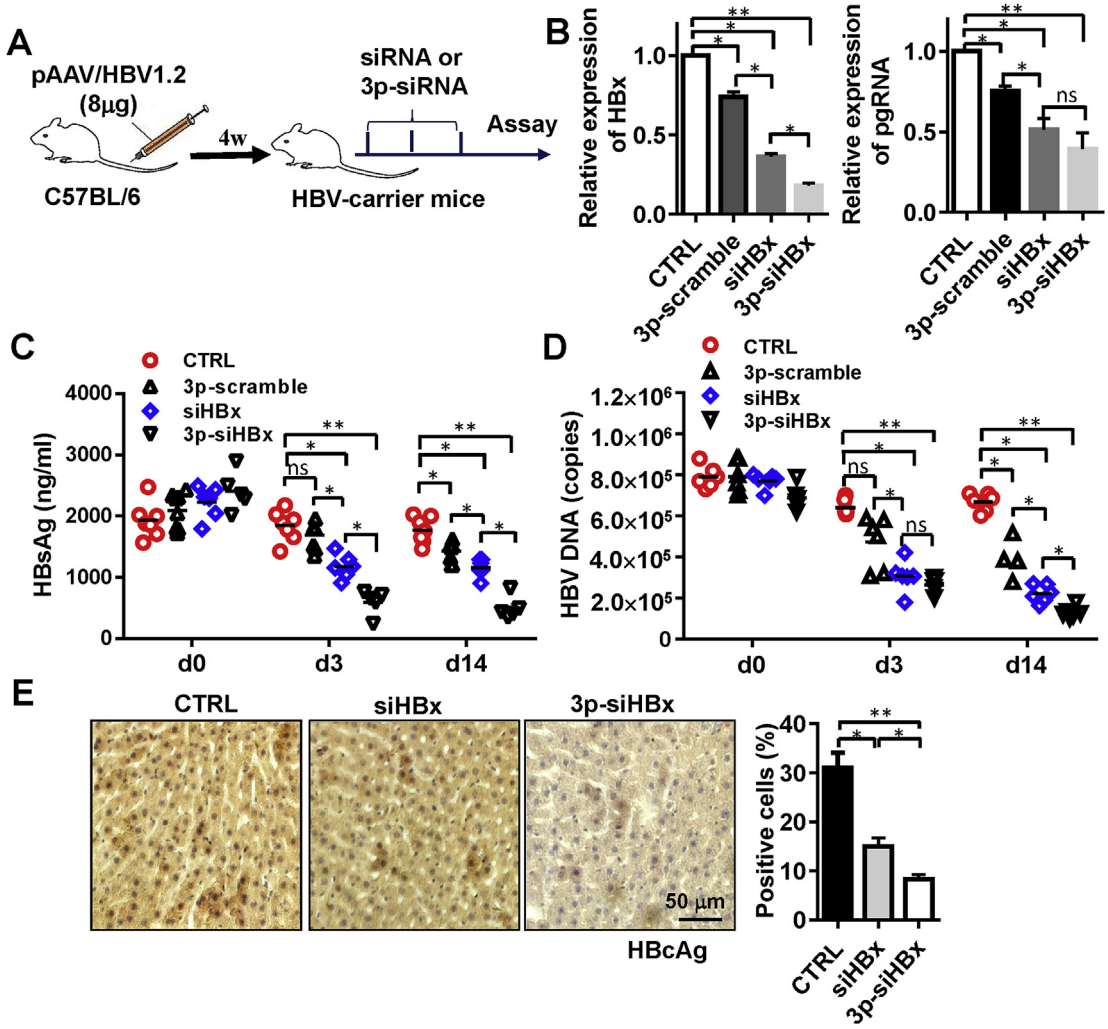

Fig. 1. 3p-siHBx inhibited HBV in HBV-carrier mice. (A) Schematic representation of HBV-carrier mice construction. pAAV/HBV1.2 plasmids were hydrodynamically injected into C57BL/6 mice, 4 weeks later, HBV-carrier mice were identified. (B–E) HBV-carrier mice (n = 6) were injected with irrelevant 3p-scramble, siHBx or 3p-siHBx every other day for three times after complexation with DOTAP. Two weeks after the last treatment, the expression of HBx and pgRNA liver tissues was detected by PCR (B) Serum HBsAg and HBV DNA copies (D) was detected by ELISA (C) and qPCR on day 0, 3 and 14 after the last treatment, respectively. (E) IHC assay of HBcAg expression in liver tissue on day 14 after the last treatment; the percentage of the HBcAg-positive cells were calculated from three fields.

T cell exhaustion.

3.4. 3p-siHBx promoted dendritic cell (DC) maturation in HBV-Carrier mice

DC maturation and activity are important for $CD8^+$ T cell activation. However, accumulating data suggest the function of pDC, including IFN-α production and costimulatory molecule expression, from chronic HBV patients are impaired significantly (Duan et al., 2005; Urcuqui-Inchima et al., 2017). Here, we observed no obvious difference in hepatic $CD11c^+$ DC proportions and total numbers among liver tissues of 3p-scramble, 3p-siHBx, siHBx-treated and DOTAP-treated mice (Fig. 4A). However, 3p-siHBx upregulated the costimulatory molecule CD80 in hepatic DCs (Fig. 4B), but did not affect CD86 or major histocompatibility complex (MHC) expression significantly (Fig. 4C&D). A similar trend of CD80 upregulation was observed in DCs from mice treated by irrelevant 3p-scramble, while siHBx treatment did not affect CD80 and CD86 of DC significantly (Fig. 4B–D). Furthermore, IFN-α was increased in DCs from HBV-carrier mice 7 days after 3p-siHBx or 3p-scramble treatment, but not in siHBx-treated mice (Fig. 4E). These results indicate that 3p-siHBx can augment DC activity in chronic HBV mice.

3.5. 3p-siHBx decreased MDSCs in chronic HBV mice

A hallmark of chronic HBV infection is the expansion of MDSCs that effectively suppresses $CD8^+$ T and NK cell responses (Fang et al., 2015). Here, we observed larger accumulation of these suppressive cells in HBV-carrier mice in comparison with pAAV-infected mice, which was significantly reversed in 3p-siHBx-injected mice; however, irrelevant 3p-scramble did not affect MDSC proportion significantly (Fig. 5A). Simultaneously, 3p-siHBx significantly and 3p-scramble slightly inhibited reactive oxygen species (ROS) production in MDSCs, but siHBx treatment did not show significant effected on ROS production (Fig. 5B). In addition, we observed the production of immunosuppressive cytokines IL-10 and TGF-β was decreased in HBV-carrier mice after 3p-siHBx treatment, while TGF-β but not IL-10 was deceased by siHBx treatment, and irrelevant 3p-scramble treatment did not affect TGF-β or IL-10 significantly (Fig. 5C). These results show that 3p-siHBx suppresses MDSC differentiation in HBV-carrier mice.

3.6. The antiviral effects of 3p-siHBx were partially mediated by RIG-I activation in vivo

RIG-I recognizes specific molecular patterns of viral RNAs with 5′-

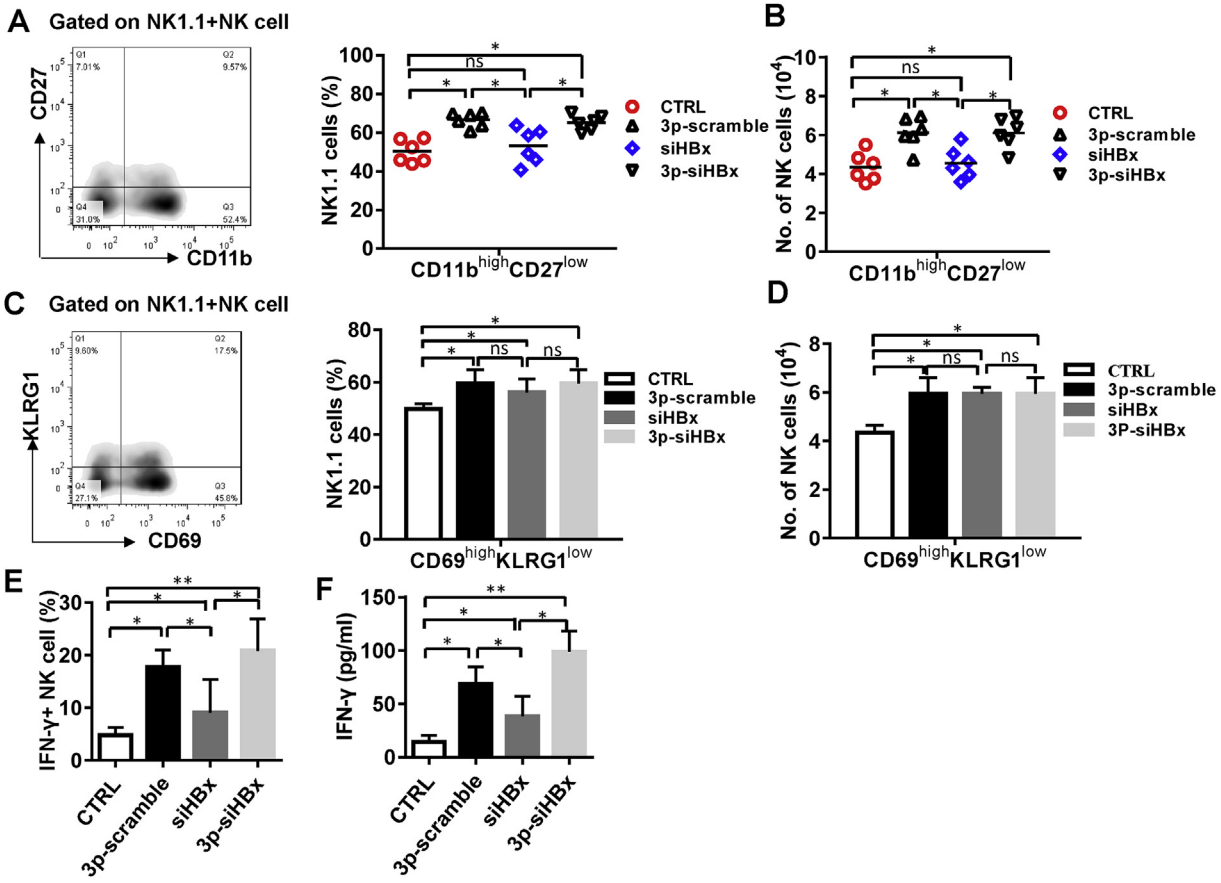

Fig. 2. 3p-siHBx activated NK cells in HBV-carrier mice. Two weeks after the last treatment, the mice were sacrificed and intrahepatic lymphocytes were isolated. (A) Representative FACS plots of $CD11b^+$ and $CD27^{low}$ $NK1.1^+$ cells in liver leukocytes (left). The percentages of NK cells according to their maturation phenotype (Right). (B) Absolute numbers of $CD11b^+CD27^{low}$ NK cells. (C) Representative FACS plots of $CD69^+$ and $KLRG1^+NK1.1^+$ cells in liver leukocytes (left). The percentages of NK cells according to CD69 and KLRG1 expression (right). (D) Absolute numbers of NK cells according to CD69 and KLRG1 expression. (E) Quantification graph of IFN-γ–producing NK cells. (F) ELISA analysis of serum IFN-γ levels. Data were obtained from 3 independent experiments with similar results (n = 6).

triphosphate (Chen et al., 2013). To determine whether the RIG-I signaling pathway was activated after 3p-siHBx treatment *in vivo*, hepatocytes were isolated from HBV-carrier mice. As shown in Fig. 6A, 3p-siHBx and 3p-scramble increased RIG-I expression in hepatocytes, while conventional siHBx did not affect RIG-I expression. IRF-3 regulates IFN-β expression and plays an important role in RIG-I–mediated antiviral immunity (Chen et al., 2013). 3p-siHBx and 3p-scramble significantly enhanced the RIG-I–mediated IRF-3 activation in hepatocytes, while siHBx exhibited a weak ability to promote IRF-3 activation (Fig. 6B, Left). Meanwhile, the activation of the two mitogen-activated protein kinases (MAPKs), ERK and p38, was increased in the hepatocytes of 3p-siHBx–treated mice, and siHBx was also found to activate p38 and ERK (Fig. 6B, Right). Moreover, 3p-siHBx and 3p-scramble led to obvious upregulation of IFN-β (Fig. 6C) and type III IFN (IFN-λ) in the liver tissue (Fig. 6D), and the expression of ISGs such as ISG15 and OAS1 (Fig. 6E). These results also demonstrate that conventional siRNA targeting HBx only induced a moderate IFN response (Fig. 6C–E). To confirm whether RIG-I activation contributed to 3p-siHBx–induced HBV inhibition, siRIG-I was administered to the HBV-carrier mice to silence RIG-I before 3p-siHBx treatment, the RNAi effect of siRIG-I was verified (Fig. 6F, left). We observed that RIG-I pre-silencing partially abrogated 3p-siHBx–induced HBx and pgRNA inhibition (Fig. 6F, right). Moreover, the level of HBsAg was partly restored in HBV-carrier mice pre-treated with siRIG-I before 3p-siHBx treatment (Fig. 6G). These results demonstrate that 3p-siHBx–induced type I and type III IFN responses and HBV inhibition depend partially on RIG-I activation *in vivo*.

3.7. 3p-siHBx enhanced T cell and NK cell infiltration

Based on the above observations, we wanted to know whether 3p-siHBx could enhance the infiltration of effector cells to improve the liver immune microenvironment. First, we determined whether 3p-siHBx could affect chemokine expression in HBV^+ HepG2. 2.15 cells. As shown in Fig. 7A, CCL2, CCL5, CCL8, and CXCL10 levels were upregulated in 3p-siHBx–transfected cells. Meanwhile, we observed the irrelevant 3p-scramble could promote the expression of these chemokines, which was similar to the effect of 3p-siHBx, while this effect induced by conventional siHBx was lower than 3p-RNA. Transwell migration assays performed to analyze immune cell infiltration *in vitro* revealed that 3p-siHBx–treated HepG2. 2.15 cells were sufficient to recruit immune cells from PBMCs (Fig. 7B). Obviously, the supernatant from 3p-siHBx–treated HepG2. 2.15 cells enhanced the T cell and NK cell recruitment (Fig. 7C). These results indicate that RIG-I activation might be important for the infiltration of activated $CD8^+$ T cells and NK cells into HBV-infected liver tissue.

4. Discussion

HBV develops several strategies to suppress antiviral immune responses. Here, we used a bifunctional siRNA molecule to silence HBx and activate RIG-I, which induced HBV inhibition partly mediated by RIG-I in HBV-carrier mice. Furthermore, this 3p-siHBx could induce DC maturation and NK cell activation, and reverse HBV-induced $CD8^+$ T cell exhaustion. These data clearly indicate that RNAi-mediated

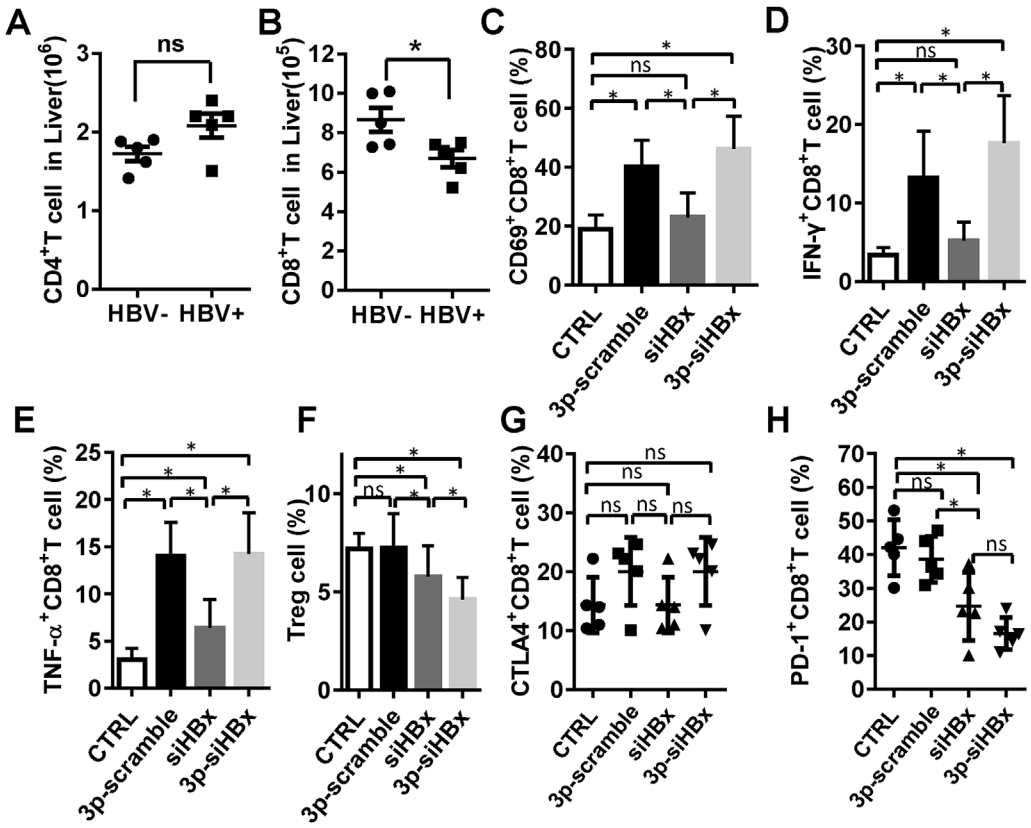

Fig. 3. 3p-siHBx induced CD8$^+$ T cell response in HBV-carrier mice. (A, B) pAAV or pAAV/HBV1.2 vector were delivered into C57BL/6 mice using the tail vein injection, 4 weeks later, intrahepatic lymphocytes were isolated. The percentage of CD4$^+$ T cells (A) and CD8$^+$ T (B) cells was detected by FACS. (C–H) HBV-carrier mice were treated by irrelevant 3p-scramble, siHBx, or 3p-siHBx every other day for three times. The percentage of CD69$^+$CD8$^+$ T cells (C), IFN-γ$^+$- (D) and TNF-α$^+$- (E) CD8$^+$ T cells, and Tregs (F), as well as CTLA-4 (G) and PD-1 (H) expression on CD8$^+$ T cell were assayed on day 14 after the last injection. CTRL, untreated HBV-carrier mice as above. Data were obtained from 3 independent experiments with similar results (n = 5).

sequence-specific degradation of HBV RNA and RIG-I responses are major antiviral mechanisms in HBV-carrier mice.

A major hurdle to treating HBV is the profound immunosuppression, both systemically and locally, within the liver immune microenvironment through different pathways (Chyuan and Hsu, 2018; Shin et al., 2016). For example, HBx disrupts the interaction between RIG-I and TRAF3 (TNF receptor–associated factor 3) and finally dampens type I IFN induction. HBV polymerase inhibits RIG-I–induced IFN-α/β induction by interfering with IRF-3 phosphorylation, dimerization, and nuclear translocation, and suppressing TBK1/IKKε (TANK-binding kinase 1/inhibitor of NF-κB kinase) and DDX3 (DEAD-box helicase 3, X-linked) interaction in human hepatocytes (Jiang and Tang, 2010; Wang et al., 2010).

RIG-I activation leads to type I IFN responses, triggering the innate and adaptive immune responses. We previously demonstrated that 3p-siHBx exerted potent anti–HBV efficacy via HBx silencing and RIG-I activation (Han et al, 2011). We found HBx-siRNA has obvious HBx silencing but weak RIG-I activation effect. On the contrary, 3p-scramble siRNA has week HBV silencing but strong RIG-I activation effect by their 5′-triphosphate structure. In addition to its direct HBx silencing, the bifunctional siRNA (3p-siHBx) exerts more inhibitory effect on HBV replication, which derived from its arousal of IFN response by activation of RIG-I pathway. The potential of bifunctional 3p-siRNAs has also been studied in several other models, including influenza A Virus, coxsackievirus, Nodamura virus infection (Fan et al., 2015; Lin et al., 2012). Also, several studies reported bifunctional 3p-siRNA (Exp:targeting Bcl 2/TGF-β/Survivin/Glutaminase/IDO/VEGF/MDR1) with target silence and stimulated innate immunity by way of RIG-I activation, could confer potent antitumor efficacy (Li et al., 2017; Meng et al., 2014; Wang et al., 2013; Yuan et al., 2015). Therefore, bifunctional 3p-siRNA is extremely attractive as a candidate for tumor or antiviral therapy.

NK cells and CD8$^+$ T cells are important effector cells in anti-HBV immune responses; however, both are impaired in the presence of chronic HBV infection. TGF-β, IL-10, MDSCs, and Tregs play immunosuppressive roles during HBV infection (Hong and Bertoletti, 2017; Li et al., 2015; Tan et al., 2015). Here, we confirmed that 3p-siHBx markedly decreased HBV load (Fig. 1). Significantly, we observed that 3p-siHBx could promote the activation of NK cells and CD8$^+$ T cells, and induce the expression of CD80 and CD86 on DCs in naïve C57BL/6 mice (sFig. 4). Subsequently, we found NK cells, particularly CD11b^{high}CD27^{low} mature NK cells, were recruited to the liver after 3p-siHBx treatment (Fig. 2). Meanwhile, the frequency of CD69^{high}KLRG1^{low} hepatic NK cells was increased in 3p-siHBx–treated HBV-carrier mice, accompanied by increased IFN-γ–producing NK cells. Furthermore, 3p-siHBx activated CD8$^+$ T cells, exhibited augmented ability to produce TNF-α and IFN-γ and decreased PD-1 expression, which is similar to the effect of irrelevant 3p-scramble treatment. Interestingly, 3p-siHBx but not 3p-scramble inhibited Treg generation and TGF-β and IL-10 production effectively (Fig. 3). More importantly, 3p-siHBx significantly induced DC maturation (Fig. 4) and reduced CD11b$^+$Gr-1$^+$ MDSC numbers, while siHBx treatment only slightly inhibited MDSC, and there is no difference in MDSC and suppressive cytokines between 3p-scramble and control group (Fig. 5). To date, there has been no report that RIG-I activation can activate B cells and promote antibody secretion. In our study, we found that 3p-siHBx did not increase anti-HBs antibodies in HBV-carrier mice (sTable.1). We surmise that the cytokines produced by the 3p-siHBx–treated hepatocytes were not sufficient to activate B cells and T follicular helper (Tfh) cells. Nevertheless, this study presents an interesting issue to be resolved in future studies. These findings all suggest that the bifunctional 3p-siHBx can reverse HBV infection–induced immune dysfunction by improving NK cell and CD8$^+$ T cell function.

It is important to note that upon RIG-I activation, IRF-3, p38, and ERK were activated by 3p-siHBx, leading to upregulated IFN response (Fig. 6). This suggests that 3p-siHBx has specific effects on HBV replication. In addition, 3p-siHBx induced type III IFN response (Fig. 6D), which could also inhibit HBV replication. We speculate that the type III

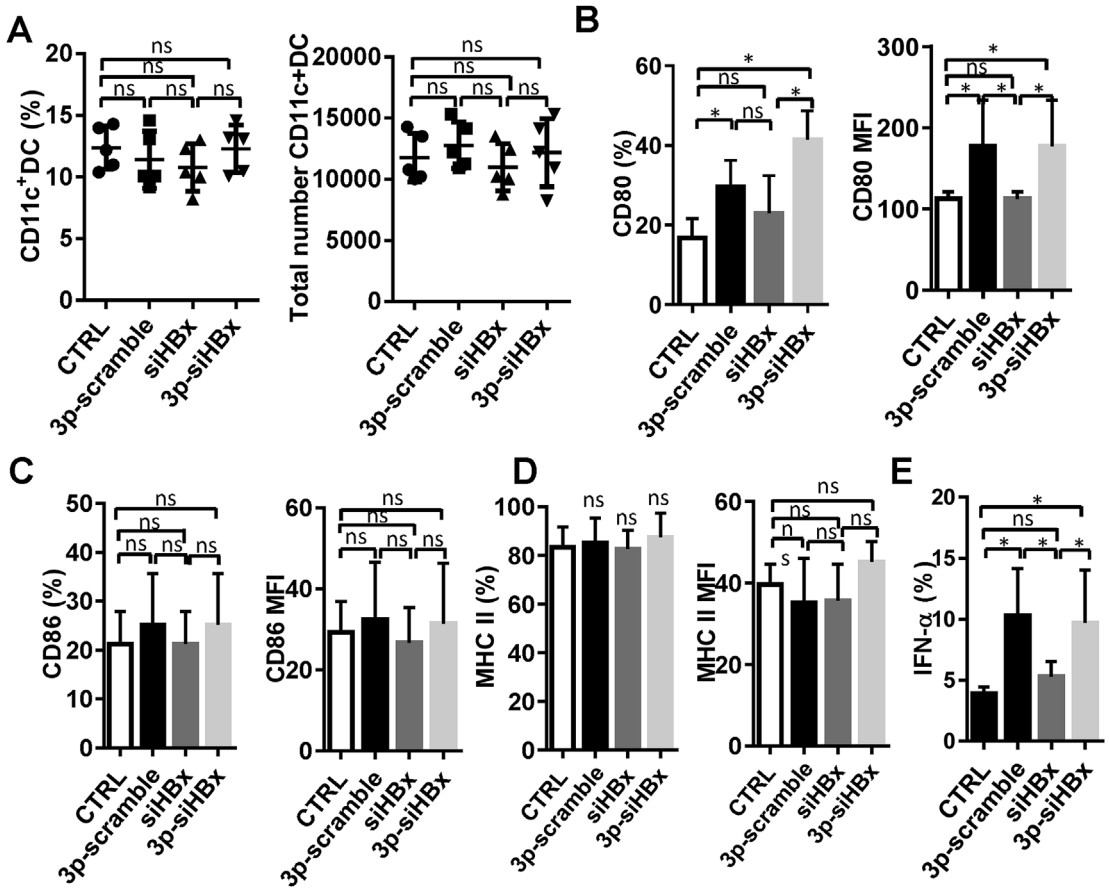

Fig. 4. 3p-siHBx induced DC maturation in HBV-carrier mice. HBV-carrier mice were sacrificed on day 14 after irrelevant 3p-scramble, siHBx, or 3p-siHBx treatment, then intrahepatic lymphocytes were isolated. (A) DC percentages (left) and absolute numbers (right) according to CD11c expression. (B–D) FACS assay of CD80 (B), CD86 (C), and MHC II (D) expression. (E) FACS assay of IFN-α production in DCs after the treatments. CTRL, HBV-carrier mice untreated as above. Data were obtained from 3 independent experiments with similar results. n = 5, ns, not significant; MFI, mean fluorescence index.

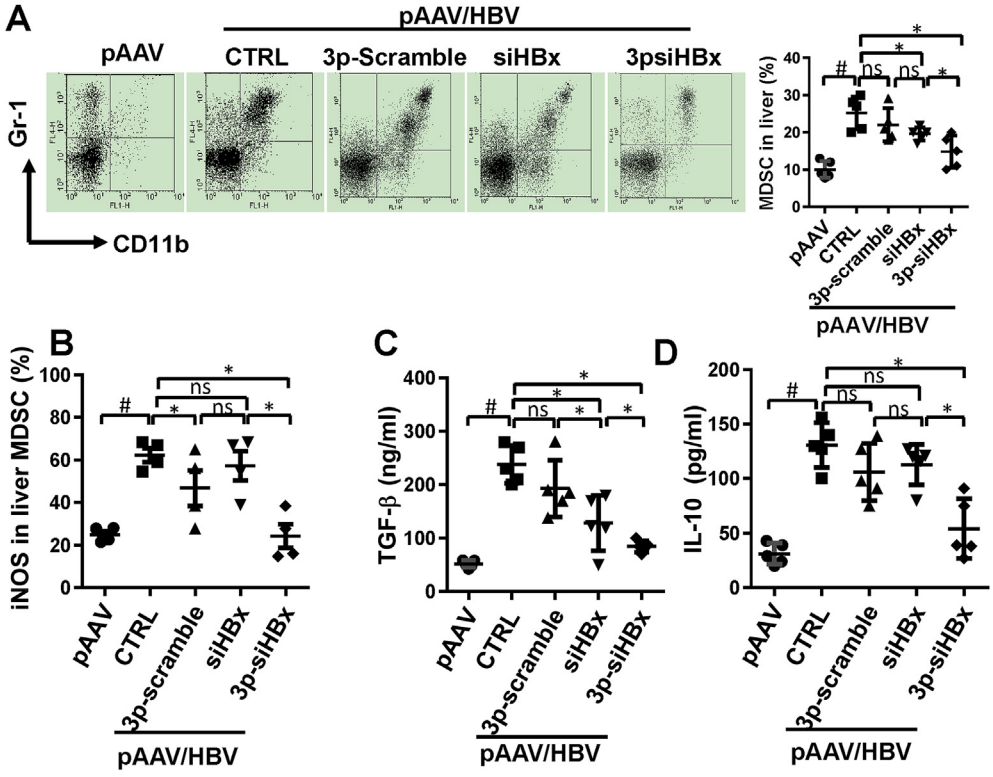

Fig. 5. 3p-siHBx inhibited MDSCs in HBV-carrier mice. Intrahepatic lymphocytes were isolated on day 14 after the last irrelevant 3p-scramble, siHBx, or 3p-siHBx treatment. (A) Representative FACS plots of $CD11b^+$ and $Gr\text{-}1^+$ MDSCs (Left). Quantification graph of MDSCs in HBV-carrier mice after treatment (Right). (B) Quantification graph of iNOS expression after 3p-siHBx treatment in HBV-carrier mice. (C, D) ELISA of serum TGF-β (C) and IL-10 (D) levels. Each dot represents an individual mouse. Data were obtained from 3 independent experiments with similar results (n = 5).

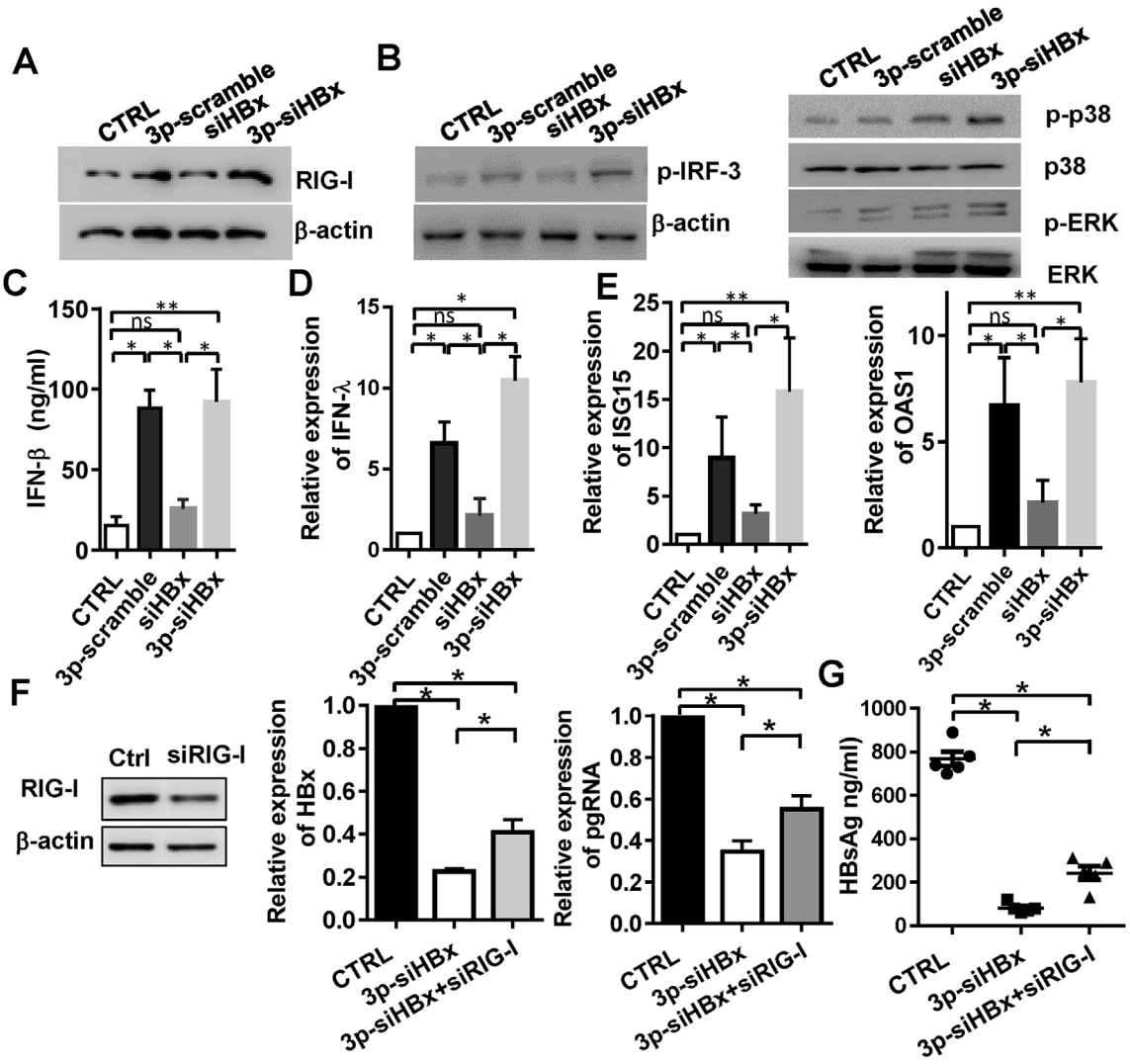

Fig. 6. HBV inhibition was partially dependent on RIG-I activation *in vivo*. (A) Western blot of RIG-I expression in liver tissues from 3p-siHBx– or siHBx-treated HBV-carrier mice. (B) Western blots of IRF (left) and MAPK (right) signals. (C) ELISA analysis of serum IFN-β levels. (D) Real-time PCR detection of IFN-λ expression in liver tissues. (E) Real-time PCR assay of ISG15 and OAS1 expression. RIG-I protein was verified after treated with siRIG-I for 24h (F, left). qPCR detection of HBx, pgRNA (F,right) and ELISA detection of HBsAg levels (G) were performed in HBV-carrier mice pre-treated with siRIG-I before 3p-siHBx treatment. Data are expressed as the mean ± SD from at least three independent experiments (n = 5).

IFN response might be partially attributed to anti-viral effect mediated by 3p-siHBx. In relation to the evaluation of the experiments shown in Fig. 6F, silencing RIG-I partially recovered HBV inhibition. Therefore, we presume that the effect of 3p-siHBx might not only base on its RNAi activity but also on RIG-I activating activity. In addition to RIG-I, previous studies have indicated that Toll-like receptor (TLR)7/8/9 or STING (transmembrane protein 173) agonists can activate the intrahepatic innate immune responses, which can control HBV infection efficiently. Therapeutic strategies based on pathogen recognition receptor (PRR) activation are intended to activate the antiviral signaling pathway that suppresses HBV replication and simultaneously reverse HBV-specific T cell exhaustion (Thursz, 2014; Urcuqui-Inchima et al., 2017). A potent and orally available TLR7 agonist (GS-9620) activated B cells, $CD8^+$ T cells, and/or NK cells and induced type I/II IFN response in the liver microenvironment (Menne et al., 2015). Moreover, ssRNA40, a TLR8 agonist, selectively activated NKT and $CD56^{bright}$ NK cells to produce IFN-γ in HBV-infected livers (Jo et al., 2014).

Interestingly, 3p-siHBx could recruit NK cells and T cells (Fig. 7); it is possible that DC mutation in PBMCs and chemokine secretion of 3p-siHBx treated HBV + hepatocytes contributed to this process. Therefore, RIG-I is likely to play dual roles as an innate sensor and as a direct antiviral effector for host defense during viral infection. Whether TLR 7/8/9 or STING activation promotes the recruitment of NK and T cells in HBV models need to be further studied.

RNAi has been widely used to interference HBV infection in basic research. As the smallest open reading frame and also the most obvious overlap on the structure of the HBV genome region, HBx is required for HBV efficient replication, thus making it a potentially useful target for antiviral therapy (Belloni et al., 2009). Nowadays, the most effective and clinically advanced siRNA delivery systems should be investigated to protect siRNA from degradation *in vivo*. And a clinical trial of ARC-520 based on RNAi surpassed expectations (Liu et al., 2016). Our study might provide a candidate strategy for the development of a nucleic acid drug for therapy of not only virus infections, including HBV, but also for different tumors. 3p-siHBx is expected to be a promising immunomodulatory drug for improving treatment efficacy by abrogating immunosuppression.

In conclusion, combining RIG-I activation with HBx silencing via a bifunctional 3p-siRNA disrupts HBV-mediated immunosuppressive mechanisms and confers potent antiviral efficacy. RIG-I is an important target for immunotherapy of HBV infection. However, the therapeutic potential of 3p-siHBx requires further evaluation in more biologically

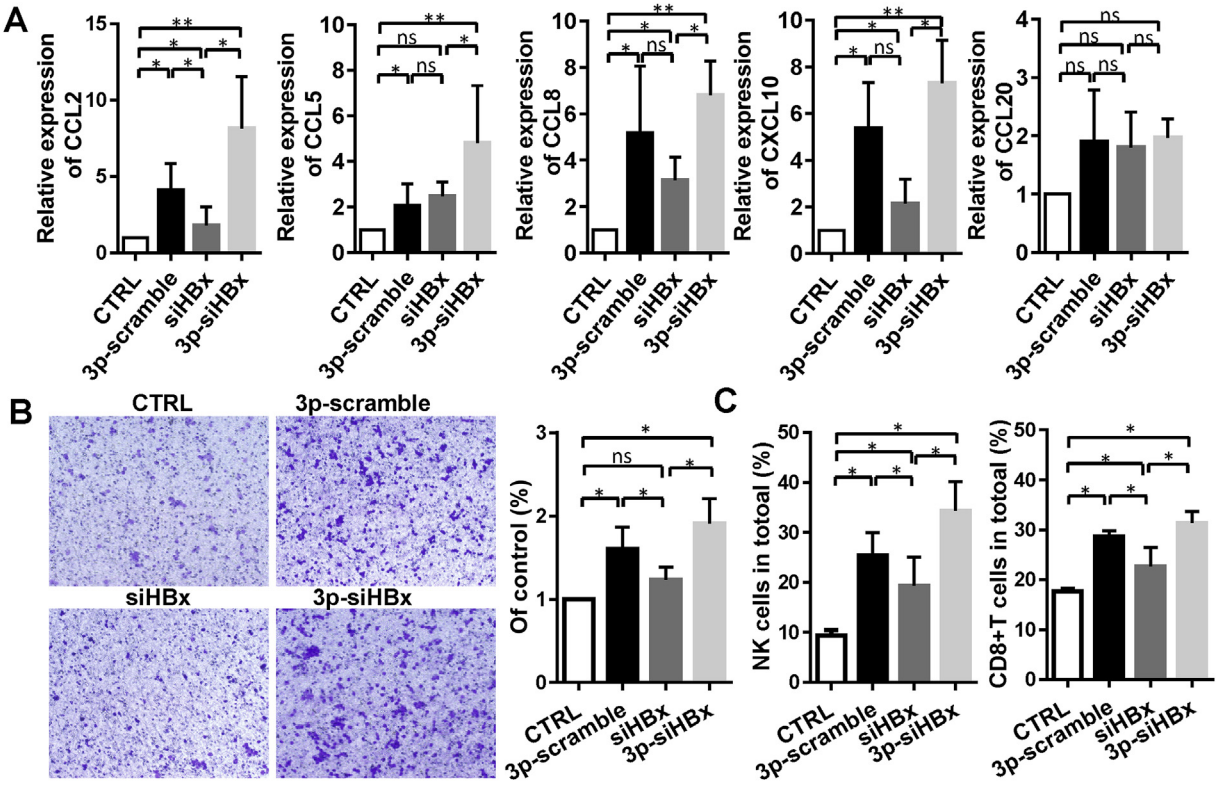

Fig. 7. 3p-siHBx recruited T cells and NK cells through chemokines. (A) Real-time RT-PCR of CCL2, CCL5, CCL8, and CXCL10 levels in HepG2. 2.15 cells transfected with 3p-siHBx, 3p-scramble or siHBx. (B) Transwell migration assay of PBMC infiltration by supernatant from HepG2. 2.15 cells-treated by different kind of RNA. Representative images were captured at random; quantitation was performed through blinded cell counting. (C) Flow cytometry determination of the percentages of immune cell subsets 6 h after co-culture. Shown is one representative result of at least three experiments. Data are expressed as the mean ± SD from at least three independent experiments.

relevant animal species and in human clinical trials.

Disclosures

The authors report no potential conflicts of interest.

Ethics approval and consent to participate

The animal research was approved by the Animal Research Ethics Committee of Shandong University and complied with the Guidelines for Animal Experiments of Laboratory Animals.

Fundings

This work was supported by Shandong Provincial Key Research and Development Program [grant number 2017GSF18159], Shandong Provincial Natural Science Foundation, China [grant number ZR2017BH029, BS2015YY023], Fundamental Research Fund of Shandong University (2017JC004), and the National Natural Science Foundation of China (grant number 81601441).

Appendix A. Supplementary data

Supplementary data to this article can be found online at https://doi.org/10.1016/j.antiviral.2018.11.006.

References

Ahn, J., Ko, A., Jun, E.J., Won, M., Kim, Y.K., Ju, E.S., Jeon, E.S., Lee, H., 2012. Antiviral effects of small interfering RNA simultaneously inducing RNA interference and type 1 interferon in coxsackievirus myocarditis. Antimicrob. Agents Chemother. 56, 3516–3523.

Anz, D., Koelzer, V.H., Moder, S., Thaler, R., Schwerd, T., Lahl, K., Sparwasser, T., Besch, R., Poeck, H., Hornung, V., Hartmann, G., Rothenfusser, S., Bourquin, C., Endres, S., 2010. Immunostimulatory RNA blocks suppression by regulatory T cells. J. Immunol. 184, 939–946.

Belloni, L., Pollicino, T., De Nicola, F., Guerrieri, F., Raffa, G., Fanciulli, M., Raimondo, G., Levrero, M., 2009. Nuclear HBx binds the HBV minichromosome and modifies the epigenetic regulation of cccDNA function. Proc. Natl. Acad. Sci. U. S. A. 106, 19975–19979.

Chen, X., Qian, Y., Yan, F., Tu, J., Yang, X., Xing, Y., Chen, Z., 2013. 5'-triphosphate-siRNA activates RIG-I-dependent type I interferon production and enhances inhibition of hepatitis B virus replication in HepG2.2.15 cells. Eur. J. Pharmacol. 721, 86–95.

Chyuan, I.T., Hsu, P.N., 2018. Tumor necrosis factor: the key to hepatitis B viral clearance. Cell. Mol. Immunol. 15, 731–733.

de Niet, A., Stelma, F., Jansen, L., Sinnige, M.J., Remmerswaal, E.B., Takkenberg, R.B., Kootstra, N.A., Reesink, H.W., van Lier, R.A., van Leeuwen, E.M., 2016. Restoration of T cell function in chronic hepatitis B patients upon treatment with interferon based combination therapy. J. Hepatol. 64, 539–546.

Duan, X.Z., Zhuang, H., Wang, M., Li, H.W., Liu, J.C., Wang, F.S., 2005. Decreased numbers and impaired function of circulating dendritic cell subsets in patients with chronic hepatitis B infection (R2). J. Gastroenterol. Hepatol. 20, 234–242.

Ebert, G., Poeck, H., Lucifora, J., Baschuk, N., Esser, K., Esposito, I., Hartmann, G., Protzer, U., 2011. 5' Triphosphorylated small interfering RNAs control replication of hepatitis B virus and induce an interferon response in human liver cells and mice. Gastroenterology 141, 696–706 706 e691-693.

Elbashir, S.M., Harborth, J., Lendeckel, W., Yalcin, A., Weber, K., Tuschl, T., 2001. Duplexes of 21-nucleotide RNAs mediate RNA interference in cultured mammalian cells. Nature 411, 494–498.

Ellermeier, J., Wei, J., Duewell, P., Hoves, S., Stieg, M.R., Adunka, T., Noerenberg, D., Anders, H.J., Mayr, D., Poeck, H., Hartmann, G., Endres, S., Schnurr, M., 2013. Therapeutic efficacy of bifunctional siRNA combining TGF-beta 1 silencing with RIG-I activation in pancreatic cancer. Cancer Res. 73, 1709–1720.

Fan, X., Dong, S., Li, Y., Ding, S.W., Wang, M., 2015. RIG-I-dependent antiviral immunity is effective against an RNA virus encoding a potent suppressor of RNAi. Biochem. Biophys. Res. Commun. 460, 1035–1040.

Fang, Z., Li, J., Yu, X., Zhang, D., Ren, G., Shi, B., Wang, C., Kosinska, A.D., Wang, S., Zhou, X., Kozlowski, M., Hu, Y., Yuan, Z., 2015. Polarization of monocytic myeloid-derived suppressor cells by hepatitis B surface antigen is mediated via ERK/IL-6/STAT3 signaling feedback and restrains the activation of T cells in chronic hepatitis B virus infection. J. Immunol. 195, 4873–4883.

Han, Q., Zhang, C., Zhang, J., Tian, Z., 2011. Reversal of hepatitis B virus-induced

immune tolerance by an immunostimulatory 3p-HBx-siRNAs in a retinoic acid inducible gene I-dependent manner. Hepatology 54, 1179–1189.
Hong, M., Bertoletti, A., 2017. Tolerance and immunity to pathogens in early life: insights from HBV infection. Semin. Immunopathol. 39, 643–652.
Huang, L.R., Wu, H.L., Chen, P.J., Chen, D.S., 2006. An immunocompetent mouse model for the tolerance of human chronic hepatitis B virus infection. Proc. Natl. Acad. Sci. U. S. A. 103, 17862–17867.
Jiang, J., Tang, H., 2010. Mechanism of inhibiting type I interferon induction by hepatitis B virus X protein. Protein Cell 1, 1106–1117.
Jo, J., Tan, A.T., Ussher, J.E., Sandalova, E., Tang, X.Z., Tan-Garcia, A., To, N., Hong, M., Chia, A., Gill, U.S., Kennedy, P.T., Tan, K.C., Lee, K.H., De Libero, G., Gehring, A.J., Willberg, C.B., Klenerman, P., Bertoletti, A., 2014. Toll-like receptor 8 agonist and bacteria trigger potent activation of innate immune cells in human liver. PLoS Pathog. 10, e1004210.
Kell, A.M., Gale Jr., M., 2015. RIG-I in RNA virus recognition. Virology 479–480, 110–121.
Lan, P., Zhang, C., Han, Q., Zhang, J., Tian, Z., 2013. Therapeutic recovery of hepatitis B virus (HBV)-induced hepatocyte-intrinsic immune defect reverses systemic adaptive immune tolerance. Hepatology 58, 73–85.
Li, D., Gale, R.P., Liu, Y., Lei, B., Wang, Y., Diao, D., Zhang, M., 2017. 5'-Triphosphate siRNA targeting MDR1 reverses multi-drug resistance and activates RIG-I-induced immune-stimulatory and apoptotic effects against human myeloid leukaemia cells. Leuk. Res. 58, 23–30.
Li, H.J., Zhai, N.C., Song, H.X., Yang, Y., Cui, A., Li, T.Y., Tu, Z.K., 2015. The role of immune cells in chronic HBV infection. J. Clin. Transl. Hepatol. 3, 277–283.
Lin, L., Liu, Q., Berube, N., Detmer, S., Zhou, Y., 2012. 5'-Triphosphate-short interfering RNA: potent inhibition of influenza A virus infection by gene silencing and RIG-I activation. J. Virol. 86, 10359–10369.
Liu, S.H., Seto, W.K., Lai, C.L., Yuen, M.F., 2016. Hepatitis B: treatment choice and monitoring for response and resistance. Expet Rev. Gastroenterol. Hepatol. 10, 697–707.
Meng, G., Xia, M., Xu, C., Yuan, D., Schnurr, M., Wei, J., 2014. Multifunctional antitumor molecule 5'-triphosphate siRNA combining glutaminase silencing and RIG-I activation. Int. J. Canc. 134, 1958–1971.
Menne, S., Tumas, D.B., Liu, K.H., Thampi, L., AlDeghaither, D., Baldwin, B.H., Bellezza, C.A., Cote, P.J., Zheng, J., Halcomb, R., Fosdick, A., Fletcher, S.P., Daffis, S., Li, L., Yue, P., Wolfgang, G.H., Tennant, B.C., 2015. Sustained efficacy and seroconversion with the Toll-like receptor 7 agonist GS-9620 in the Woodchuck model of chronic hepatitis B. J. Hepatol. 62, 1237–1245.
Poeck, H., Besch, R., Maihoefer, C., Renn, M., Tormo, D., Morskaya, S.S., Kirschnek, S., Gaffal, E., Landsberg, J., Hellmuth, J., Schmidt, A., Anz, D., Bscheider, M., Schwerd, T., Berking, C., Bourquin, C., Kalinke, U., Kremmer, E., Kato, H., Akira, S., Meyers, R., Hacker, G., Neuenhahn, M., Busch, D., Ruland, J., Rothenfusser, S., Prinz, M., Hornung, V., Endres, S., Tuting, T., Hartmann, G., 2008. 5'-Triphosphate-siRNA: turning gene silencing and Rig-I activation against melanoma. Nat. Med. 14, 1256–1263.
Schlee, M., Roth, A., Hornung, V., Hagmann, C.A., Wimmenauer, V., Barchet, W., Coch, C., Janke, M., Mihailovic, A., Wardle, G., Juranek, S., Kato, H., Kawai, T., Poeck, H., Fitzgerald, K.A., Takeuchi, O., Akira, S., Tuschl, T., Latz, E., Ludwig, J., Hartmann, G., 2009. Recognition of 5' triphosphate by RIG-I helicase requires short blunt double-stranded RNA as contained in panhandle of negative-strand virus. Immunity 31, 25–34.
Schmidt, A., Schwerd, T., Hamm, W., Hellmuth, J.C., Cui, S., Wenzel, M., Hoffmann, F.S., Michallet, M.C., Besch, R., Hopfner, K.P., Endres, S., Rothenfusser, S., 2009. 5'-triphosphate RNA requires base-paired structures to activate antiviral signaling via RIG-I. Proc. Natl. Acad. Sci. U. S. A. 106, 12067–12072.
Schuch, A., Hoh, A., Thimme, R., 2014. The role of natural killer cells and CD8(+) T cells in hepatitis B virus infection. Front. Immunol. 5, 258.
Shin, E.C., Sung, P.S., Park, S.H., 2016. Immune responses and immunopathology in acute and chronic viral hepatitis. Nat. Rev. Immunol. 16, 509–523.
Tan, A., Koh, S., Bertoletti, A., 2015. Immune response in hepatitis B virus infection. Cold Spring Harb. Perspect. Med. 5, a021428.
Thursz, M., 2014. Basis of HBV persistence and new treatment options. Hepatol. Int. 8 (Suppl. 2), 486–491.
Urcuqui-Inchima, S., Cabrera, J., Haenni, A.L., 2017. Interplay between dengue virus and Toll-like receptors, RIG-I/MDA5 and microRNAs: implications for pathogenesis. Antivir. Res. 147, 47–57.
Wang, K., Chen, X., Yan, F., Xing, Y., Yang, X., Tu, J., Chen, Z., 2013. 5'-triphosphate-siRNA against survivin gene induces interferon production and inhibits proliferation of lung cancer cells in vitro. J. Immunother. 36, 294–304.
Wang, X., Li, Y., Mao, A., Li, C., Li, Y., Tien, P., 2010. Hepatitis B virus X protein suppresses virus-triggered IRF3 activation and IFN-beta induction by disrupting the VISA-associated complex. Cell. Mol. Immunol. 7, 341–348.
Wu, S.F., Wang, W.J., Gao, Y.Q., 2015. Natural killer cells in hepatitis B virus infection. Braz. J. Infect. Dis. 19, 417–425.
Yang, Y., Han, Q., Hou, Z., Zhang, C., Tian, Z., Zhang, J., 2017. Exosomes mediate hepatitis B virus (HBV) transmission and NK-cell dysfunction. Cell. Mol. Immunol. 14, 465–475.
Yoneyama, M., Fujita, T., 2009. RNA recognition and signal transduction by RIG-I-like receptors. Immunol. Rev. 227, 54–65.
Yuan, D., Xia, M., Meng, G., Xu, C., Song, Y., Wei, J., 2015. Anti-angiogenic efficacy of 5'-triphosphate siRNA combining VEGF silencing and RIG-I activation in NSCLCs. Oncotarget 6, 29664–29674.